Table I. Geometric Comparison of Three Tetranuclear Platinum Blue Related Compounds

compd	color	av Pt ox. state	Pt-Pt, Å	Pt-Pt-Pt, deg	ref
1	blue	2.25	2.774 2.877	164.60	5, 6
2	dark red	2.50	2.702 2.709	170.44 168.75	*a*
3	greenish yellow	2.0	2.88 3.13		10

[a] This work.

a class of compounds called under the generic name "platinum blues" seem to be due to the differences of the average platinum oxidation state, and the present study revealed the characteristic nature of these compounds—they are oligomeric amidate-bridged platinum compounds, whose platinum oxidation state changes to various degrees without basic structural change. This nature resembles that of one-dimensional platinum chain compounds. Platinum blues might be a suitable class of compounds for the study of Pt–Pt interactions of the chain compounds in the solution phase.

The differences of the platinum oxidation states in the three compounds are also reflected in the Pt–Pt distances, as shown in Table I. The Pt–Pt distance of the three tetranuclear complexes increases as the Pt oxidation state decreases, a correlation similar to that observed for one-dimensional platinum complexes.[11,12] Other examples of bridged platinum(II) or platinum(III) dimers and their Pt–Pt distances are as follows: 3.229 and 3.11 Å in *cis*-diammineplatinum(II) pyrophosphate dimer,[13] 2.97 Å in *cis*-diammineplatinum(II) 1-methylthyminato head-to-tail dimer,[14] 2.91 Å in *cis*-diammineplatinum(II) 1-methylthyminato head-to-head dimer,[15] 2.90 Å in *cis*-diammineplatinum(II) α-pyridone head-to-tail dimer,[10] and 2.466 Å in sulfate-bridged Pt(III)–Pt(III) dimer.[16] These values for bridged Pt–Pt complexes are somewhat shorter than those found in the nonbridged one-dimensional compounds with corresponding oxidation states as pointed out earlier.[5] Moreover, we should also note the recently reported very interesting example of bridged platinum compound, *cis*-nitrodiammineplatinum 1-methylcytosinato head-to-tail dimer,[17] whose platinum oxidation state is also 2.5 and the Pt–Pt distance is 2.584 Å. Each of the platinum atoms in this compound is definitely coordinated by a nitro group (Pt–N = 2.12 and 2.13 Å) in the axial position and accordingly can be considered as six-coordinated. This situation is markedly different from that of the present compound; the platinum atoms in the present compound are very loosely coordinated by nitrate groups at both ends of the Pt chain and the Pt–O (nitrate anion) distances are larger than 3 Å. The Pt–Pt distances (2.702 and 2.709 Å) are significantly larger than that of 1-methylcytosinato dimer. Therefore, Pt–Pt distances seem to be related to how the platinum atoms are coordinated in the axial position as well as to the platinum oxidation state. In order to discuss fully these relations and the factors which determine the Pt–Pt distance, further confirmation of the platinum oxidation state with other methods such as oxidation–reduction titration or susceptibility measurement are desired.[18] Such experiments are now under way. The Pt–Pt chain is not straight in any platinum blue related compounds. The Pt–Pt–Pt angles are summarized in Table I, and the angles in the present compound (**2**), 170.4 and 168.8°, are somewhat larger than those found in platinum α-pyridone blue. To answer the question whether this zigzag chain angles have any correlation with the platinum oxidation state, we have to await the detailed report on compound **3**. The platinum coordination planes are canted to each other. The angles between the planes are 18.68° between Pt1 and Pt2 and 21.22° between Pt3 and Pt4, while the coordination planes for Pt2 and Pt3 are almost parallel; the angle between them is 1.01°. This canting feature is quite similar to that of α-pyridone blue and is the result of the fact that N···O bite distances of α-pyrrolidone ligand (av 2.40 Å) is shorter than Pt–Pt bond length (2.70 Å). Other details of the structure and solution properties will be published later.

Acknowledgment. This work was supported by a grant for a development of anticancer medicines (No. 23665) from the Japanese Ministry of Health and Welfare.

Supplementary Material Available: Atomic positional and thermal parameters for compound **2** (2 pages). Ordering information is given on any current masthead page.

(11) Williams, J. M. *Inorg. Nucl. Chem. Lett.* **1976**, *12*, 651.

(12) Reis, A. H., Jr.; Peterson, S. W. *Inorg. Chem.* **1976**, *15*, 3186.

(13) Stanko, J. A.; Cleare, M. J. In "Platinum Coordination Complexes in Chemotherapy"; Connors, T. A., Roberts, J. J., Ed.; Springer-Verlag: New York, 1974; pp 24–26.

(14) Lock, C. J. L.; Peresie, H. J.; Rosenberg, B.; Turner, G. *J. Am. Chem. Soc.* **1978**, *100*, 3371.

(15) Lippert, B.; Neugebauer, D.; Schubert, U. *Inorg. Chim. Acta* **1980**, *46* (B1), L11.

(16) Maraveiskaya, G. S.; Kukina, G. A.; Orlova, V. S.; Evstafeva, O. N.; Porai-Koshits, M. A. *Dokl. Akad. Nauk. SSSR* **1976**, *226*, 596.

(17) Faggiani, R.; Lippert, B.; Lock, C. J. L.; Speranzini, R. A. *J. Am. Chem. Soc.* **1981**, *103*, 1111.

(18) Although we considered the possibility that the present complex may contain the pentahydrodioxonium cation as seen in the platinum pyrimidine monomer or dimer complexes (see ref 17 and 19), we cannot definitely say whether such an oxonium cation exists in the present compound, since, as mentioned in ref 9, there seems to be some disorder in the crystal lattice. If the compound contains such an oxonium cation, the platinum oxidation state must be changed to a lower value, and in that case, the relation between the Pt–Pt distance and the platinum oxidation state of the present compound would be nearer to that of platinum 1-methylcytosinato dimer. The formula $(H_5O_2)[Pt_4(NH_4)_8(C_4H_6ON)_4](NO_3)_6 \cdot H_2O$, whose average platinum oxidation state is 2.25, also gives almost identical calculated elemental concentrations (C, 11.44; H, 3.31; N, 15.01; Pt, 46.44%) with the proposed formula, but as we could not find any definite oxonium cation in the final difference map, we have chosen the proposed formula.

(19) Faggiani, R.; Lippert, B.; Lock, C. J. L. *Inorg. Chem.* **1980**, *19*, 295.

Photochemistry of Surface-Confined Mononuclear and Trinuclear Ruthenium Carbonyl Complexes. Direct Evidence for the Ability To Isolate Photogenerated Intermediates from Each Other on High Surface Area Silica

David K. Liu and Mark S. Wrighton*

Department of Chemistry
Massachusetts Institute of Technology
Cambridge, Massachusetts 02139

Received October 23, 1981

Photoactivation of homogeneous organometallic catalysts by light-induced extrusion of 2-electron donor ligands or metal–metal bond cleavage has been demonstrated.[1-5] A problem that has

(1) (a) Geoffroy, G. L.; Wrighton, M. S. "Organometallic Photochemistry"; Academic Press: New York, 1979. (b) Graff, J. L.; Sanner, R. D.; Wrighton, M. S. *J. Am. Chem. Soc.* **1979**, *101*, 273. (c) Mitchener, J. C.; Wrighton, M. S. *Ibid.* **1981**, *103*, 975. (d) Wrighton, M. S.; Graff, J. L.; Reichel, C. L.; Sanner, R. D. *Ann. N. Y. Acad. Sci.* **1980**, *333*, 188. (e) Austin, R. G.; Paonessa, R. S.; Giordano, P. J.; Wrighton, M. S. *Adv. Chem. Ser.* **1978**, *No. 168*, 189.

(2) King, A. D., Jr.; King, R. B.; Sailers, E. L., III. *J. Am. Chem. Soc.* **1981**, *103*, 1867.

(3) Chase, D. B.; Weigert, F. J. *J. Am. Chem. Soc.* **1981**, *103*, 977.

(4) Balzani, V.; Carassiti, V. "Photochemistry of Coordination Compounds"; Academic Press: New York, 1970.

(5) (a) Platbrood, G.; Wilputte-Steinert, L. *J. Organomet. Chem.* **1974**, *70*, 393, 407; **1975**, *85*, 199. *Tetrahedron Lett.* **1974**, 2507. (b) Nasielski, J.; Kirsch, P.; Wilputte-Steinert, L. *J. Organomet. Chem.* **1971**, *27*, C13. (c) Krausz, P.; Carnier, F.; DuBois, J. E. *J. Am. Chem. Soc.* **1975**, *97*, 437. (d) Agapiou, A.; McNelis, E. *J. Chem. Soc., Chem. Commun.* **1975**, *187*. *J. Organomet. Chem.* **1975**, *99*, C47.

0002-7863/82/1504-0898$01.25/0

Table I. Spectroscopic Data for Relevant Compounds[a]

compd	IR ν_{CO}, cm^{-1} (ϵ or relative o.d.)	UV–vis λ_{max}, nm (ϵ)
$Ru(CO)_4(PPh_2Me)$	2060 (2710), 1984 (1810), 1946 (4860)	254 (9150)[b] (absorption)
$[(EtO)_3SiCH_2CH_2PPh_2]Ru(CO)_4$	2058 (2800), 1982 (1350), 1946 (4840)	257 (9190)[b] (absorption)
$[(EtO)_3SiCH_2CH_2PPh_2]Ru(CO)_3PPh_3$	1896 (5040)	
$[(EtO)_3SiCH_2CH_2PPh_2]Ru(CO)_3(P(OCH_2)_3CCH_2CH_3)$	1917	
$[S]-LRu(CO)_4$[c]	2059 (1.0), 1995 (1.0), 1952 (0.6)	255 (photoacoustic)
$[S]-LRu(CO)_3(PPh_3)$	1900 (1.0)	
$[S]-LRu(CO)_3(P(OCH_2)_3CCH_2CH_3)$[d]	1920 (1.0)	
$Ru_3(CO)_9(PPh_2Me)_3$	2042 (320), 1970 (2800), 1943 (1510)	484 (13 600), 364 (sh) (absorption)
$[(EtO)_3SiCH_2CH_2PPh_2]_3Ru_3(CO)_9$	2044 (240), 1970 (2790), 1940 (850)	488 (13 200), 366 (sh) (absorption)
$[S]-L_3Ru_3(CO)_9$	2056 (0.8), 1988 (1.0), 1950 (sh), 2066 (0.8),[e] 2004 (1.0),[e] 1965 (sh)[e]	490, 370 (sh) (photoacoustic)

[a] All measurements were made in toluene solution at 25 °C for soluble Ru complexes by using conventional techniques. For the surface-confined species infrared spectra were typically recorded as Nujol mulls by Fourier transform infrared spectrometer (Nicolet 7199), and UV–visible absorption data were obtained by using a Cary 17 for soluble species, and photoacoustic spectra were obtained by using a PAR 6001 PAS spectrometer for powders. [b] Measured in hexane solution at 25 °C. [c] Prepared via reaction 4 or from irradiation of $[S]-L_3Ru_3(CO)_9$ under CO. [d] Generated from either $[S]-LRu(CO)_4$ or $[S]-L_3Ru_3(CO)_9$ irradiated in the presence of $P(OCH_2)_3CCH_2CH_3$. [e] Measured in a KBr pellet.

arisen is that the reactive solution species can recombine with the extruded ligand or can react with each other to form inactive clusters.[1] We now report the synthesis and photochemical behavior of $LRu(CO)_4$ and $L_3Ru_3(CO)_9$ confined to the surface of high surface area silica. The results illustrate that immobilization of precursors to coordinatively unsaturated species prevents cluster formation when the surface coverage is sufficiently low. Further, photodeclusterification of anchored $L_3Ru_3(CO)_9$ is reversible due to the immobilization of the fragments.

Reactions 1–4, each having precedence in the literature,[1b,6-8]

$$Ru_3(CO)_{12} \xrightarrow[(EtO)_3SiCH_2CH_2PPh_2]{60\ ^\circ C} [(EtO)_3SiCH_2CH_2PPh_2]_3Ru_3(CO)_9 \quad (1)^{6,7}$$

$$[(EtO)_3SiCH_2CH_2PPh_2]_3Ru_3(CO)_9 \xrightarrow[[S]-OH]{25\ ^\circ C} [S]-L_3Ru_3(CO)_9 + 9EtOH \quad (2)^8$$

$$[(EtO)_3SiCH_2CH_2PPh_2]_3Ru_3(CO)_9 \xrightarrow[CO,\ 1\ atm]{h\nu} [(EtO)_3SiCH_2CH_2PPh_2]Ru(CO)_4 \quad (3)^{1b,6,7}$$

$$[(EtO)_3SiCH_2CH_2PPh_2]Ru(CO)_4 \xrightarrow[[S]-OH]{25\ ^\circ C} [S]-LRu(CO)_4 + 3EtOH \quad (4)^8$$

outline the procedure used to anchor $LRu(CO)_4$ and $L_3Ru_3(CO)_9$ to the surface of high surface area, 400 m^2/g, SiO_2 (Alfa).[9] The key to the preparation of the surface-confined $LRu(CO)_4$ and $L_3Ru_3(CO)_9$ is to use the phosphine ligand $(EtO)_3SiCH_2CH_2PPh_2$ (Strem) to prepare the derivatives of $Ru_3(CO)_{12}$; similar reagents have been prepared by using PPh_2Me as structural and spectral models (Table I).[6,7] The $(EtO)_3Si-$ functionality allows the covalent attachment of the Ru species to the SiO_2 surface via reaction with surface OH groups.[8] We use $[S]-LRu(CO)_4$ and $[S]-L_3Ru_3(CO)_9$ to represent the two systems. Infrared and UV–VIS spectra (Table I) and elemental analyses clearly establish that metal carbonyl moieties can be confined to SiO_2. There is a rather significant change in the relative intensities of the infrared features upon reaction to anchor $Ru(CO)_4L$ and $Ru_3(CO)_9L_3$ to the surface. Metal carbonyl absorptions in the CO stretching region are very sensitive to local structure. The UV–VIS spectra of the $[S]-LRu(CO)_4$ and $[S]-L_3Ru_3(CO)_9$ accord well with solution absorption spectra of $Ru(CO)_4L$ and $Ru_3(CO)_9L_3$ (Table I). From elemental analyses the key elements, Ru and P, are present in a ratio, $\sim 1/1$, that is consistent with the retention of the species claimed.[10] From the analyses the coverage ($\sim 3 \times 10^{-11}$ mol/cm^2) is less than what would be regarded as a monolayer ($\sim 10^{-10}$ mol/cm^2), assuming that the coverage is uniform. Since the anchoring group is $(EtO)_3Si-$, the Ru species may be anchored to the surface in polymeric amounts,[8] but the low coverage tends to rule out extensive polymerization. We shall assume that the coverage is uniform and that extensive polymerization does not occur. Photochemical results described below are consistent with this assumption.

Paralleling results reported earlier for $Ru(CO)_4PPh_3$ and $Ru_3(CO)_9(PPh_3)_3$,[1b] the photochemistry of $[(EtO)_3SiCH_2CH_2PPh_2]Ru(CO)_4$ and $[(EtO)_3SiCH_2CH_2PPh_2]_3Ru_3(CO)_9$, are represented by reactions 5–7.[11] The results

$$[(EtO)_3SiCH_2CH_2PPh_2]Ru(CO)_4 \xrightarrow[L' = PPh_3,\ ^{13}CO,\ P(OCH_2)_3CCH_2CH_3]{355 \pm 20\ nm} [(EtO)_3SiCH_2CH_2PPh_2]Ru(CO)_3L' + CO \quad (5)$$

$$[(EtO)_3SiCH_2CH_2PPh_2]Ru(CO)_4 \xrightarrow[toluene,\ N_2\ purge]{355 \pm 20\ nm} {}^1/_3[(EtO)_3SiCH_2CH_2PPh_2]_3Ru_3(CO)_9 + CO \quad (6)$$

$$[(EtO)_3SiCH_2CH_2PPh_2]_3Ru_3(CO)_9 \xrightarrow[L' = P(OCH_2)_3CCH_2CH_3,\ PPh_3,\ CO]{436\ nm} 3[(EtO)_3SiCH_2CH_2PPh_2]Ru(CO)_3L' \quad (7)$$

are consistent with dissociative loss of CO from the $Ru(CO)_4L$ (L = PPh_3, PPh_2R (R = alkyl)) species; the quantum yield at 366 nm is 0.40 ± 0.05 for reaction according to (5) for L′ = PPh_3, $P(OCH_2)_3CCH_2CH_3$ at 0.1 M in degassed toluene solution at 25 °C. The photoreaction of $Ru_3(CO)_9L_3$ is consistent with Ru–Ru

(6) Johnson, B. F. G.; Lewis, J.; Twigg, M. V. *J. Chem. Soc., Dalton Trans.* **1976**, 1876.

(7) Johnson, B. F. G.; Lewis, J.; Twigg, M. V. *J. Organomet. Chem.* **1974**, *67*, C75.

(8) (a) Bailey, D. C.; Langer, S. H. *Chem. Rev.* **1981**, *81*, 109. (b) Hartley, F. R.; Vezey, P. N. *Adv. Organomet. Chem.* **1977**, *15*, 189.

(9) High surface area SiO_2 (400 m^2/g) purchased from Alfa was pretreated by heating at ~250 °C under vacuum (10^{-2} torr) for 48 h. A typical preparation of $[S]-LRu(CO)_4$ (yellow) or $[S]-L_3Ru_3(CO)_9$ (red) involves the suspension of ~1 g of pretreated SiO_2 in toluene. Excess $[(EtO)_3SiCH_2CH_2PPh_2]Ru(CO)_4$ or $[(EtO)_3SiCH_2CH_2PPh_2]_3Ru_3(CO)_9$ is added and the suspension stirred at 25 °C for 24 h under N_2. The solid is collected by filtration and washed repeatedly with toluene, dried under vacuum, and stored under N_2. Control experiments using $Ru(CO)_4PPh_2Me$ or $Ru_3(CO)_9(PPh_2Me)_3$ as the derivatizing reagents yield no surface-confined metal carbonyls, yielding only white, underivatized SiO_2 after washing with toluene.

(10) The elemental analysis of $[S]-LRu(CO)_4$ is 1.57% Ru and 0.39% P (percentages are by weight), giving an atom ratio Ru/P close to the expected 1:1. The coverage is thus 3.9×10^{-11} mol/cm^2, assuming the surface area to be 400 m^2/g. The elemental analysis of $[S]-L_3Ru_3(CO)_9$ is 3.29% Ru and 0.95% P, again giving a Ru/P atom ratio close to the expected 1:1 and a coverage of 2.7×10^{-11} mol/cm^2. Elemental analyses were performed by Galbraith Laboratories.

(11) Irradiations were carried out by using a GE Black Lite for 355 ± 20 nm or a Hanovia 450-W medium pressure Hg lamp with Corning glass filters to isolate the 366- or 436-nm emission.

Scheme I. Representations of the Photochemistry of [S]-$Ru(CO)_4$ and [S]-$L_3Ru_3(CO)_9$

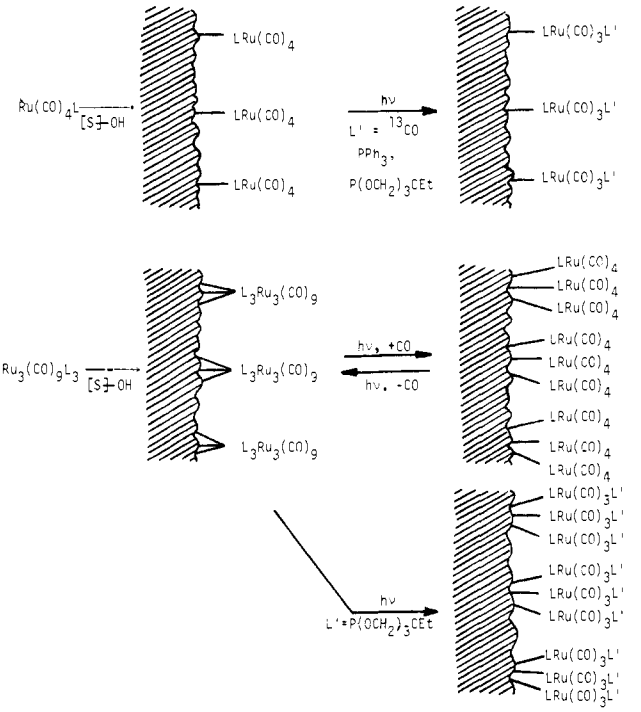

bond cleavage as the prompt result of excited-state decay. The quantum yield for the reaction represented by reaction 7 at an L′ concentration of 0.1 M in toluene is $\sim 10^{-3}$ for 436-nm excitation. Fortunately, the $Ru_3(CO)_9L_3$ species absorb at lower energy [λ_{max} ~490 nm, (ϵ 14 000)] than do the $Ru(CO)_4L$ species [λ_{max} ~260 nm (ϵ 9000)], allowing completely selective excitation of the $Ru_3(CO)_9L_3$ in the presence of large concentrations of $Ru(CO)_4L$.

Irradiation of [S]-$LRu(CO)_4$ and [S]-$L_3Ru_3(CO)_9$ suspended in degassed isooctane solutions results in chemical changes consistent with dissociative loss of CO from the mononuclear species and metal–metal bond cleavage of the trinuclear species. Scheme I summarizes the chemistry that has been done. Irradiation of [S]-$LRu(CO)_4$ suspended in degassed isooctane containing 0.05 M PPh_3 or $P(OCH_2)_3CCH_2CH_3$ gives infrared spectral changes consistent with the formation of [S]-$LRu(CO)_3L'$, where L and L′ are trans, axial ligands as in the $Ru(CO)_3LL'$ complexes (Table I), since there is only one infrared absorption in the CO stretching region. The key fact is that the spectral changes accompanying the irradiation of [S]-$LRu(CO)_4$ in the presence of L′ reveal a single CO stretch at a position very close to that for $[(EtO)_3SiCH_2CH_2PPh_2]Ru(CO)_3L'$ formed photochemically. The conversion is clean and gives a good yield of the [S]-$LRu(CO)_3L'$ based on the relative absorptivities of $Ru(CO)_4L$ and $Ru(CO)_3LL'$. The irradiation of [S]-$L_3Ru_3(CO)_9$ in the presence of L′ = $P(OCH_2)_3CCH_2CH_3$ yields an infrared spectral change to give a single CO stretch in exactly the same position as for [S]-$LRu(CO)_3L'$ formed by irradiation of [S]-$LRu(CO)_4$. Thus, the surface-confined cluster appears to undergo metal–metal bond cleavage upon photoexcitation, paralleling the solution analogue.

An important finding relates to the photochemistry of the [S]-$LRu(CO)_4$ formed from irradiation of [S]-$L_3Ru_3(CO)_9$ under CO. As illustrated in Figure 1, 436-nm irradiation of [S]-$L_3Ru_3(CO)_9$ under 1 atm CO yields a spectrum identical with that for [S]-$LRu(CO)_4$ synthesized according to reaction 4. The key finding is that 355-nm irradiation of the photogenerated [S]-$LRu(CO)_4$ while purging out CO leads to the nearly quantitative regeneration of the [S]-$L_3Ru_3(CO)_9$. In sharp contrast, 355-nm irradiation of [S]-$LRu(CO)_4$ formed by the procedure in reaction 4 yields loss of all metal carbonyl absorptions under the same conditions, and we find no evidence for the formation of [S]-$L_3Ru_3(CO)_9$. The difference, as illustrated in Scheme I, is that [S]-$LRu(CO)_4$ from synthesis by reaction 4 yields -$Ru(CO)_4$ centers that are statistically far apart from each other compared to the -$Ru(CO)_4$ center from the 436-nm irradiation of [S]-$L_3Ru_3(CO)_9$ under CO. The nearly quantitative photochemical disassembly–reassembly of the [S]-$L_3Ru_3(CO)_9$ system establishes several important facts: (1) the -$Ru(CO)_4$ centers formed photochemically are immobile, remaining close enough to each other to reform the original cluster by photochemical extrusion of CO; (2) each Ru of the Ru_3 species is anchored to the surface via the $\geq SiCH_2CH_2PPh_2$ ligand; otherwise the recovery of [S]-$L_3Ru_3(CO)_9$ would be poor; (3) the -$Ru(CO)_4$ centers attached according to reaction 4 are sufficiently isolated to prevent cluster formation even though CO is ejected photochemically (Figure 1); thus, photogenerated 16-valence-electron [S]-$LRu(CO)_3$ species can be persistently isolated from each other when the coverage is dilute. In no case do we find photochemical extrusion of Ru carbonyl species into the hydrocarbon solution; the Ru–P bond is photochemically inert, as reported earlier for $Ru(CO)_4PPh_3$ and related complexes.[1b]

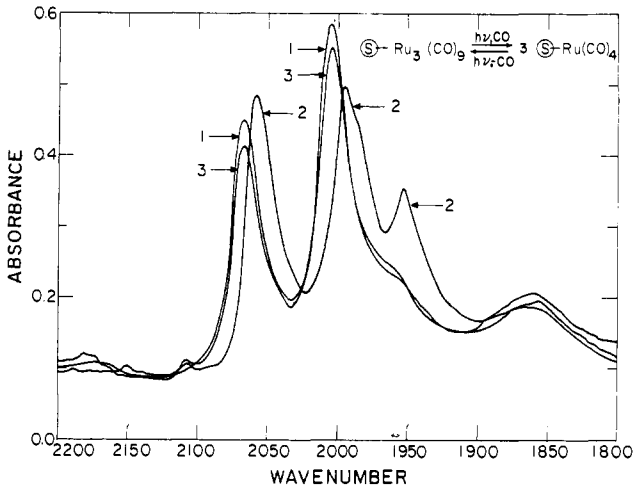

Figure 1. Representation of infrared spectral changes associated with the 436-nm irradiation of [S]-$L_3Ru_3(CO)_9$ (1) under 1 atm of CO, suspended in isooctane to yield [S]-$LRu(CO)_4$ (2). The irradiation of the photogenerated [S]-$LRu(CO)_4$ for 10 h with (355 ± 20)-nm light while purging the isooctane suspension with N_2 leads to the nearly quantitative regeneration of [S]-$L_3Ru_3(CO)_9$, spectrum 3. Spectra are for [S]-$LRu(CO)_4$/[S]-$L_3Ru_3(CO)_9$ in KBr pellets typically prepared by intimate mixing of 0.01 g of the powder with 3.0 g of KBr. Pellets of ~0.4 g are pressed at 20 000 psi to give 1.0-cm diameter, ~0.4-mm thick disks.

The photochemistry of [S]-$L_3Ru_3(CO)_9$ departs from that of its solution analogue in that irradiation in the presence of L′ = PPh_3 fails to produce [S]-$LRu(CO)_3L'$ as would be expected on the basis of the ability to photochemically form $[(EtO)_3SiCH_2CH_2PPh_2]Ru(CO)_3L'$ from the trinuclear species. However, irradiation of [S]-$L_3Ru_3(CO)_9$ in the presence of L′ = CO or $P(OCH_2)_3CCH_2CH_3$ rapidly and cleanly yields [S]-$LRu(CO)_3L'$. The conclusion is that the closely spaced, immobilized Ru atoms in [S]-$L_3Ru_3(CO)_9$ are much more structurally demanding, precluding reaction with a large ligand such as PPh_3 (cone angle = 145°)[11] whereas a small ligand like CO or $P(OCH_2)_3CCH_2CH_3$ (cone angle $\simeq$ 100°)[12] can yield mononuclear products. Preliminary studies show that [S]-$LRu(CO)_4$ and [S]-$L_3Ru_3(CO)_9$ each yield different distributions of alkene photocatalysis products under isomerization[1b] or hydrosilation conditions[1c] compared to their solution analogues, consistent with different structural demands at the photogenerated sites. These results will be reported subsequently.

Acknowledgment. We thank the Office of Naval Research and the Dow Chemical Company for partial support of this research. Support for the Nicolet 7199 Fourier transform infrared spec-

(12) Tolman, C. A. *Chem. Rev.* **1977**, *77* 313.

trometer used in these studies was provided by NIH Grant GM27551.

Registry No. $[(EtO)_3SiCH_2CH_2PPh_2]Ru(CO)_4$, 80441-14-1; $[(EtO)_3SiCH_2CH_2PPh_2]_3Ru_3(CO)_9$, 80447-60-5; SiO_2, 7631-86-9; $Ru(CO)_4(PPh_2Me)$, 57894-45-8; $[(EtO)_3SiCH_2CH_2PPh_2]Ru(CO)_3PPh_3$, 80441-15-2; $[(EtO)_3SiCH_2CH_2PPh_2]Ru(CO)_3(P(OCH_2)_3CCH_2CH_3)$, 80441-16-3; $Ru_3(CO)_9(PPh_2Me)_3$, 38686-56-5.

Gas-Phase Reactions of Certain Nucleophiles with Alkyl Trifluoroacetates. A New Probe To Distinguish between S_N2 and E2 Mechanisms for Alkyl Derivatives

Richard N. McDonald* and A. Kasem Chowdhury

Department of Chemistry, Kansas State University Manhattan, Kansas 66506

Received July 6, 1981

The gas-phase reactions of methyl trifluoroacetate with several nucleophiles appeared to proceed exclusively by the most exoergic reaction channel available, an S_N2 displacement by the nucleophile on the methyl carbon and formation of $CF_3CO_2^-$ (reaction 1).[1,2]

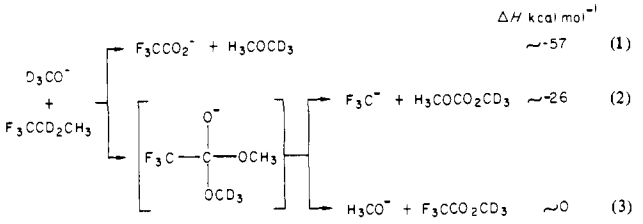

Reactions 2 and 3 illustrate two other potential product-forming channels for the reaction of D_3CO^- with $F_3CCO_2CH_3$; formation of H_3CO^- (reaction 3) was not observed.[1] When this reaction, using H_3CO^-, was repeated in our flowing in afterglow (FA) apparatus (conditions: helium buffer gas, $P_{He} = 0.5$ torr, $\bar{v} = 80$ m s^{-1}, 298 K)[3] to determine the rate constant [$(1.7 \pm 0.2) \pm 10^{-9}$ cm^3 molecule^{-1} s^{-1}], we observed that small amounts of F_3C^- (m/z 69) were produced, going through a maximum (10% of total product signals) in the early stages of the reaction.[4] We wish to report our preliminary results of the related gas-phase reactions of allyl anion with F_3CCO_2R, R = CH_3, C_2H_5, and t-C_4H_9, which establish that (a) *both* displacement on R and carbonyl addition are competitive, product-forming channels, (b) another pathway yielding F_3C^- is the decomposition of excited $F_3CCO_2^-$ formed in highly exoergic nucleophilic displacement processes, and (c) the decomposition of excited $F_3CCO_2^- \rightarrow F_3C^- + CO_2$ (and related decompositions) is useful to distinguish between S_N2 displacement vs. E2 elimination mechanisms in the reactions of C_2H_5X substrates with anions.

To enable us to identify both competitive displacement and addition reaction pathways and to insure that F_3C^- could not reasonably be formed by decomposition of the carbonyl addition adduct, we have used allyl anion[5] ($C_3H_5^-$) as the nucleophile. $C_3H_5^-$ is kinetically a good nucleophile in its reactions with H_3CX compounds,[6] and the anionic decomposition products from the addition adduct **1** (R = CH_3) would be the delocalized enolate anions $H_2C{=}CH{-}CH{=}C(-O^-)CF_3$ and/or $H_2C{=}CH{-}CH{=}C(-O^-)OCH_3$ formed by loss of CH_3OH and F_3CH, respectively[7] (discussed below).

The reaction of $C_3H_5^-$ with $F_3CCO_2CH_3$ occurred with essentially every collision, $k = (1.7 \pm 0.1) \times 10^{-9}$ cm^3 molecule^{-1} s^{-1}.[9a] The final anion reaction products (addition of 2.4×10^{11} molecules cm^{-3} of ester, $P_{He} = 0.5$ torr, $\bar{v} = 80$ m s^{-1}, 298 K)[3] were $F_3CCO_2^-$ (m/z 113), F_3C^- (m/z 69), $H_2C{=}CHCH{=}C(-O^-)OCH_3$ (m/z 99), $H_2C{=}CHCH{=}C(-O^-)CF_3$ (m/z 137), and $(F_3C)_2C(-O^-)OCH_3$ (m/z 197) in the ratio of 55:23:8:7:7, respectively. From the plot of log ion signal vs. $[F_3CCO_2CH_3]$ added to the flow, it was obvious that the amount of F_3C^- went through an early maximum and then decreased to give the above final results. This was separately shown to be the result of a fast reaction of F_3C^- with $F_3CCO_2CH_3$ [$k = (1.1 \pm 0.1) \times 10^{-9}$ cm^3 molecule^{-1} s^{-1}],[9b] giving a 2:1 ratio of $F_3CCO_2^-$ (m/z 113) and the addition adduct $(F_3C)_2C(-O^-)OCH_3$ (m/z 197). These results lead to the reaction channels formulated in reactions 4-9. That the amount of adduct m/z 197 was only 13%

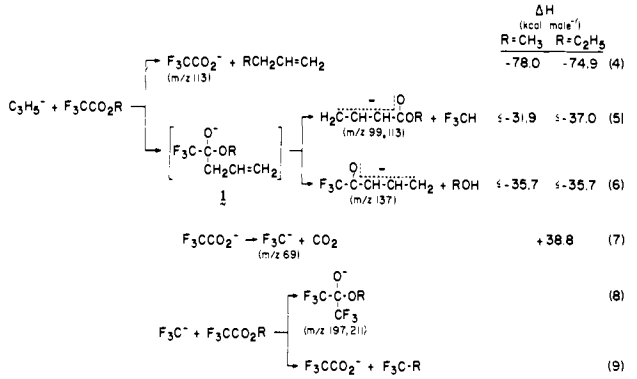

of the signal for m/z 113 from the reaction of $C_3H_5^-$ with $F_3CCO_2CH_3$ while it was 50% of m/z 113 in the reaction of F_3C^- with $F_3CCO_2CH_3$ is consistent with stepwise formation of excited $F_3CCO_2^-$ followed by competitive decomposition (yielding F_3C^- and CO_2) and third-body (He) collisional stabilization.

The reaction of $C_3H_5^-$ with $F_3CCO_2C_2H_5$ was also fast [$k = (1.5 \pm 0.1) \times 10^{-9}$ cm^3 molecule^{-1} s^{-1}].[9a] The final ion products were F_3C^- (m/z 69), $H_2C{=}CHCH{=}C(-O^-)CF_3$ (m/z 137), $F_3CCO_2^-$ (m/z 113), and $(CF_3)_2C(-O^-)OC_2H_5$ (m/z 211) in a ratio of 32:27:24:17, respectively, under the same conditions given above for the reaction of the methyl ester. (Note the differences in this ratio and that of the methyl ester and the absence of $H_2C{=}CHCH{=}C(-O^-)OC_2H_5$.[10]) As in the case of the reaction of the methyl ester, the ion signal for F_3C^- (m/z 69) was observed to go through an early maximum. The followup reaction of F_3C^- with $F_3CCO_2C_2H_5$ was separately determined, $k = (9.1 \pm 0.3) \times 10^{-10}$ cm^3 molecule^{-1} s^{-1},[9b] and gave an inverted ratio of 0.1 for the products $F_3CCO_2^-$ (m/z 113) and the adduct $(F_3C)_2C(-O^-)OC_2H_5$ (m/z 211). While reactions 4 and 6-9 (R = C_2H_5) apply to formation of these products, we must also consider the E2 elimination mechanism (reaction 10) for the formation of $F_3CCO_2^-$ from this ethyl ester.

(1) Comisarow (Comisarow, M. *Can. J. Chem.* **1977**, *55*, 171) was not explicit in the mechanism by which $CF_3CO_2^-$ was formed.

(2) Olmstead, W. N.; Brauman, J. I. *J. Am. Chem. Soc.* **1977**, *99*, 4219.

(3) McDonald, R. N.; Chowdhury, A. K.; Setser, D. W. *J. Am. Chem. Soc.* **1980**, *102*, 6491.

(4) Formation of small amounts of F_3C^- was observed early in the reaction $H_2N^- + F_3CCO_2H \rightarrow F_3CCO_2^- + NH_3$, $\Delta H = -80$ kcal mol^{-1}, but not in the reaction $F^- + F_3CCO_2CH_3 \rightarrow F_3CCO_2^- + FCH_3$, $\Delta H = -43$ kcal mol^{-1}.

(5) Allyl anion was produced in the upstream end of the flow tube by the reactions (a) $H_2N^- + CH_3CH{=}CH_2$ and (b) $F^- + (H_3C)_3SiCH_2CH{=}CH_2$ (DePuy, C. H.; Bierbaum, V. M.; Flipping, L. A.; Grabowski, J. J.; King, G. K.; Schmitt, R. J.; Sullivan, S. A. *J. Am. Chem. Soc.* **1980**, *102*, 5012.

(6) $C_3H_5^- + CH_3Br \rightarrow Br^- + 1$-butene, $k = (7.7 \pm 0.3) \times 10^{-10}$ cm^3 molecule^{-1} s^{-1}; $C_3H_5^- + CH_3Cl \rightarrow Cl^- + 1$-butene, $k = (2.9 \pm 0.1) \times 10^{-10}$ cm^3 molecule^{-1} s^{-1}.

(7) The $\Delta H°_{acid}$'s of the vinylogues $F_3CC(=O)CH_2CH{=}CH_2$ (≤340 kcal mol^{-1}) and $H_2C{=}CHCH_2CO_2CH_3$ (≤361 kcal mol^{-1}) are estimated to be ≥10 kcal mol^{-1} lower than those of $F_3CC(=O)CH_3$ (350 kcal mol^{-1}) and $H_3CCO_2CH_3$ (371 kcal mol^{-1}),[8] respectively; $\Delta H°_{acid}(F_3CH) = 376$ kcal mol^{-1} and $\Delta H°_{acid}(H_3COH) = 379$ kcal mol^{-1}.[8] Decomposition of adduct **1** is favored by ≥15 kcal mol^{-1} to yield $H_2C{=}CHCH{=}C(-O^-)OR + HCF_3$ rather than F_3C^- + ester.

(8) Bartness, J. E.; McIver, R. T. "Gas Phase Ion Chemistry"; Bowers, M. T., Ed., Academic Press: New York, 1979; Vol. 2, Chapter 11.

(9) Collision limit rate constants are calculated by the average dipole orientation theory (Su, T.; Bowers, M. T. *J. Chem. Phys.* **1973**, *58*, 3027. *Int. J. Mass. Spectrom. Ion Phys.* **1973**, *12*, 374): (a) $k_{ADO} = 2.1 \times 10^{-9}$ cm^3 molecule^{-1} s^{-1} for the reactions of $C_3H_5^-$ with these three esters. (b) $k_{ADO} = 1.8 \times 10^{-9}$ cm^3 molecule^{-1} s^{-1} for the reactions of F_3C^- with either ester.

(10) Although both $F_3CCO_2^-$ and $H_2C{=}CH{-}CH{=}C(O^-)OC_2H_5$ are m/z 113, the (M + 1) (m/z 114) ion clearly shows that m/z 113 is only $F_3CCO_2^-$.

0002-7863/82/1504-0901$01.25/0